Investigation of thermo-electro-optic properties of some mixed nematic liquid crystals

Mustafa Okumuş

Investigation of thermo-electro-optic properties of some mixed nematic liquid crystals

Mustafa Okumuş

Metallurgical and Materials Engineering, Batman University, Batman, Turkey

ABSTRACT

The 6CB/8CB/8OCB liquid crystal mixture has been studied by Differential Scanning Calorimetry (DSC), polarised optic microscopy (POM), Semiconductor Characterization System, and Ultra-violet spectrophotometry (UV). DSC and POM results indicate that the 6CB/8CB/8OCB mixture exhibits liquid crystalline properties. The capacitance-voltage and conductance-voltage measurements were performed in the frequency range of 200-500 kHz and in the temperature range of 30oC–50oC. The 6CB/8CB/8OCB mixture showed an extremely large positive dielectric anisotropy. The molar absorptivity ε for the 6CB/8CB/8OCB mixture was calculated and found to be higher than the absorptivity values of the binary mixtures due to the alkyl chain length with H-aggregation.
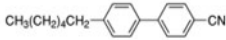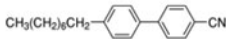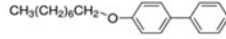
1. Introduction

Liquid crystals have a lot of interests that come from their technological applications, such as calculators, clocks, flat panel televisions, portable telephones, notebooks, and laptop computers [1–4]. Liquid crystals also have played an essential role for developing the nanotechnology and nanoscience over the last decades, such as the synthesis and design of nanomaterials using liquid crystal mesogens [5,6]. The main properties of liquid crystals are their thermal stability and dielectric anisotropy, and their knowledges are important because the upper limits of their applications may be administered by them. Phase transition behaviors and dielectric effects provide the basis for liquid crystal applications. Therefore, this treatise of the thermo-electro-optical properties of nematic liquid crystal mixtures has substantial significance in technological applications [7]. Lots of liquid crystals used in applications are eutectic mixtures of two or more mesogenic substances. The investigation of thermo-electro-optical properties of nematic liquid crystal mixtures will considerably benefit the determination of physical properties in these materials [8]. The design of technological devices and, even more important, the up-scaling from laboratory experiments to industrial processes call for detailed knowledge of the properties of the liquid crystal mixtures.

The thermo-electro-optical properties of liquid crystals can be developed by mixing of different liquid crystals or organic materials. So, the purpose of this article is to create the liquid crystal mixture materials with superior properties in many ways to be used in today's technology and to examine the characteristics of the new formation. This paper focuses on

Figure 1. Chemical structures of 4-hexyl-4′-biphenylcarbonitrile (6CB), 4′-octyl-4-biphenylcarbonitrile (8CB), and 4′-octyloxy-4-biphenylcarbonitrile (8OCB).

the mixtures of the nematogenic homologous p-(*n*-alkyl)-p′-cyanobiphenyl (*n*CB) and p-(*n*-alkoxy)-p′-cyanobiphenyl (*n*OCB), where *n* is the number of carbons in the *n*-alkyl or *n*-alkyloxy tails. Alkylcyanobiphenyl and alkoxycyanobiphenyl liquid crystals are the materials of interest in research due to their rich thermo-electro-optic properties [9–13]. In particular, liquid crystals 4-hexyl-4'-cyanobiphenyl (6CB), 4-octyl-4′-cyanobiphenyl (8CB), and 4-octyloxy-4′-cyanobiphenyl (8OCB) with a convenient temperature range of the nematic phase and good chemical stability [14] are some of the best-known liquid crystalline substances. 6CB, 8CB, and 8OCB, as well as other members of the *n*CB and *n*OCB homologous series, are very important for technological applications.

2. Experimental

2.1. *Materials*

The liquid crystal materials 4-hexyl-4'-cyanobiphenyl (6CB), 4-octyl-4′-cyanobiphenyl (8CB), and 4-octyloxy-4′-cyanobiphenyl (8OCB) were purchased from Sigma-Aldrich Corporation and were used without further purification: their phase transition temperatures were in substantial agreement with the data given in Catalogue. The structural formula of 6CB, 8CB, and 8OCB nematic liquid crystals used in this study is shown in Fig. 1.

2.2. *Thermal analysis*

The thermal properties of liquid crystal samples were measured by a Perkin-Elmer Differential Scanning Calorimeter (DSC–7) using continuous heating under a pure argon atmosphere. In order to ensure Indium (99.999 wt% pure In) was used to calibrate the DSC unit for reliable temperature and enthalpy of transition to standard values. These experiments were carried out in the −35 °C to 75 °C regions with scanning rate of 10 °C min^{-1} by means of DSC unit equipped with a Data acquisition and analysis station.

Liquid crystal samples were weighed and then stirred with an injector-needle at temperatures below T_{NI} (nematic to isotropic) transition and above T_{NI} by heating on a heating plate. This process was made carefully twice about at 30 min to ensure a complete homogenous structure. After that DSC samples were prepared in a thin aluminum pan, it was then placed on the stage of a piston-like sample crimper. The DSC was initially cooled to −35 °C, and each sample was left in the sample pan for 2 min to ensure that thermal equilibrium was reached. Then the temperature was run from −35 °C to 75 °C above its reported [15] clearing point and held at that temperatures for about 2 min to be sure of its complete transformation to the isotropic phase.

2.3. *Determination of dielectric anisotropy*

The liquid crystals 6CB, 8CB, and 8OCB to be used in the indium tin oxide (ITO) coated liquid crystal cell were weighed at equal ratios (1:1:1%wt) and they were subjected to heat treatment on the heating table after they were mixed at room temperature. The heated sample was mixed until it completely passes isotropic by using mechanical stirring methods. After the formation of a homogenous mixture, the prepared sample was immediately filled in 8.069 μm thickness cell consisting of two ITO coated conducting glass substrates by capillary reaction. The capacitance–voltage (C–V) and conductance–voltage (G–V) measurements were performed by using a Keithley 4200-SCS semiconductor analyzer.

2.4. *UV spectroscopy*

By stirring on a magnetic stirrer at a temperature below the transition temperature T_{NI} of liquid crystal mixture, the chloroform with the samples taken from the liquid crystal mixture prepared in equal proportions, homogeneous solutions within the concentration range 1.32×10^{-5} and 2.93×10^{-5} M were prepared for UV experiments. Absorption measurements were carried out at room temperature between 200 and 400 nm wavelength range by a Perkin-Elmer Lambda 45 UV/vis spectrophotometer with two 1 cm quartz cuvettes. A cuvette was filled with the solution and placed in the sample compartment of the spectrophotometer, with an identical cuvette filled with the pure solvent in the reference beam of the instrument. The intensities of light transmitted by the two cuvettes are compared automatically as the spectrometer reads over the chosen wavelength span. Before starting in situated transmission measurements, auto-zero count was taken using two cuvettes.

3. Results and discussion

Liquid crystal mixtures are used to develop the thermo-electro-optical properties of the material in LCD applications. With this in mind, I investigated the thermo-electro-optical properties of the pure 6CB, 8CB, 8OCB and their different mixtures produced in equal ratios by wt%. In literatures [16–21], some physical properties of pure 6CB, 8CB, 8OCB and their binary mixtures were investigated. However, there is no detailed study on the ternary mixtures of the liquid crystals. Thus, DSC heating cycles were performed primarily on the 6CB/8CB/8OCB mixture to determine whether it shows liquid crystalline properties.

Figure 2 shows the DSC traces of the 6CB/8CB/8OCB mixture exhibiting three endothermic peaks, indicating that the structural transformation to the isotropic phase takes place in three steps. As Fig. 2 indicates, the DSC was unsuitable to measure temperatures below −30 °C. For this reason, the phase transition temperature T_{CrA} (crystalline-smectic A) was not measured for the 6CB/8CB/8OCB mixture. The DSC spectrals for the 6CB/8CB/8OCB mixture obtained on heating across the smectic A-to-smectic C (T_{AC}), smectic C-to-nematic (T_{CN}), and nematic-to-isotropic (T_{NI}) transition temperatures are shown in Fig. 2. The DSC results indicate that the 6CB/8CB/8OCB mixture exhibits the liquid crystalline properties.

Table 1 illustrates crystal-smectic A, T_{CrA}, crystal-nematic, T_{CrN}, smectic A-smectic C, T_{AC}, smectic A-nematic, T_{AN}, smectic C-nematic, T_{CN}, nematic-isotropic, T_{NI}, phase transition temperatures and nematic range widths of ternary mixtures obtained from DSC results. As seen in Table 1, 6CB/8CB/8OCB mixture produced at 1:1:1 ratio among the pure liquid crystals and their mixtures was liquid crystal mixture having the widest nematic range with
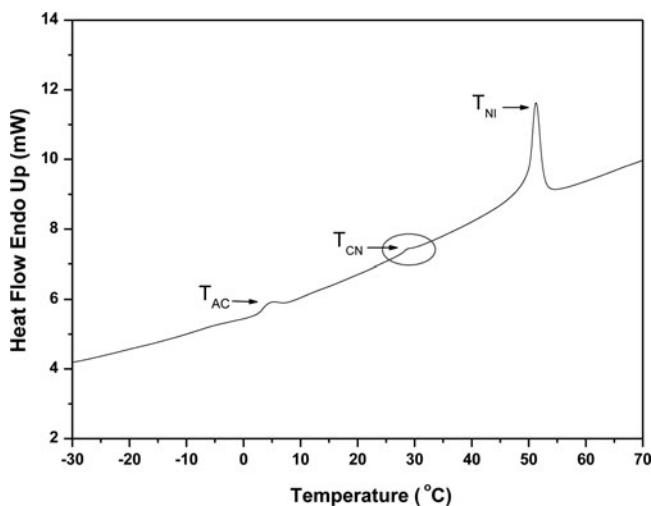
Figure 2. DSC traces obtained during continuous heating of 6CB/8CB/8OCB liquid crystal mixture at rate of 10 °C min⁻¹.

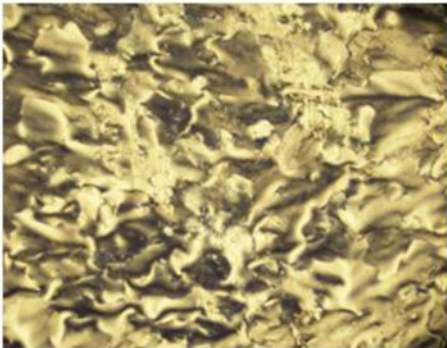22.55 °C (51.34–28.79). Furthermore, smectic C phase observed in 6CB/8CB/8OCB mixture was not observed in pure liquid crystals 6CB, 8CB, 8OCB and their binary mixtures.

Phase transition temperatures and morphological structures of 6CB/8CB/8OCB mixture were also examined using a heating table and control unit in conjunction with a polarized optic microscopy (POM). The phase transitions of 6CB/8CB/8OCB mixture observed during the heating by DSC are also observed with POM experiments. Phase identification is made according to the results of POM analysis and the standard textures reported in the literature [22]. Figure 3 shows the phase textures of 6CB/8CB/8OCB liquid crystal mixture observed during the heating by POM. Moreover, it is observed that the phase transition temperatures observed during the POM experiments are in line with the phase transition temperatures obtained in the DSC experiments.

Figure 4 illustrates the plots of capacitance–voltage of the 6CB/8CB/8OCB mixture for $\Delta\varepsilon > 0$ at different frequencies and temperatures. The capacitance values increase from the initial value $C_\perp$ to the final value $C_\parallel$. The plots indicate a threshold voltage called as Frederiks threshold voltage. Frederiks threshold voltage is a crucial parameter for any electro-optical applications of liquid crystal materials. This transition is the result of the competition between two orientational effects, which are the orientations of the director field at the boundary and due to an external electrical field. The applied electric field to LC induces a torque on the molecules due to the dielectric anisotropy and a competition with the elastic torque comes out [23]. As seen in Fig. 4, the threshold voltage and capacitance values of 6CB/8CB/8OCB

**Table 1.** The phase transition peak temperatures (*T*) of the pure liquid crystals and their mixtures.

LC and mixture	T_{CrA} (°C)	T_{CrN} (°C)	T_{AC} (°C)	T_{AN} (°C)	T_{CN} (°C)	T_{NI} (°C)	Nematic range (°C)
6CB	–	13.49	–	–	–	28.61	15.12
8CB	21.8	–	–	32.83	–	39.9	7.07
8OCB	53.54	–	–	65.25	–	78.53	13.28
6CB/8CB	–	–	–	16.68	–	36.67	19.99
6CB/8OCB	–	–	–	51.26	–	54.49	3.23
8CB/8OCB	27.27	–	–	48.05	–	58.62	10.57
6CB/8CB/8OCB	–	–	5.03	–	28.79	51.34	22.55

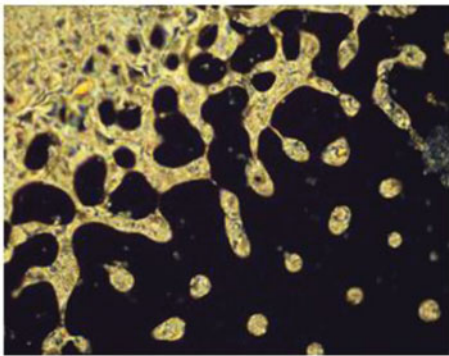The smectic A to smectic C transition at 5 °C.
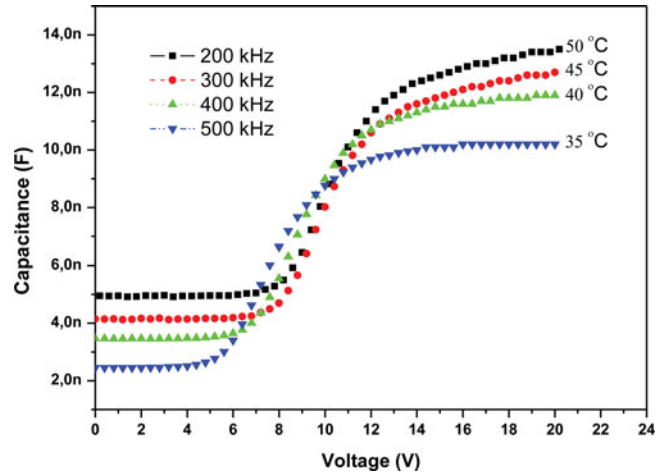
The schlieren smectic C texture at 20 °C.
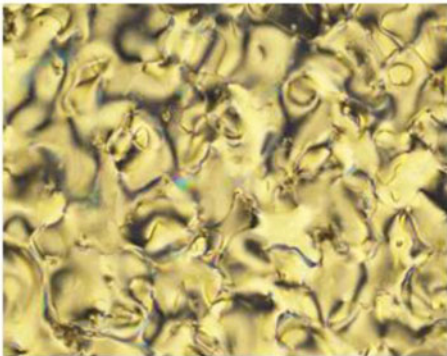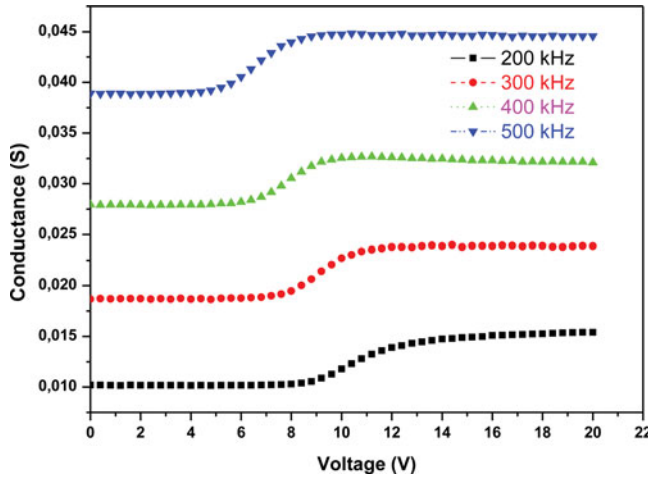
The nematic texture at 40 °C.

The nematic to isotropic transition at 51 °C.

Figure 3. Morphologic textures of 6CB/8CB/8OCB liquid crystal mixture during continuous heating by POM.

Figure 4. Capacitance–voltage (C–V) plots of the 6CB/8CB/8OCB liquid crystal mixture at different frequencies and temperatures.

Figure 5. Conductance–voltage plots of the 6CB/8CB/8OCB liquid crystal mixture at different frequencies.

mixture decrease by increasing the voltage frequency applied. Also, as temperatures increase, reorientation is challenged to become steady above the threshold voltage. In the temperature range of the nematic phase, the threshold voltage is about 6 V. However, the threshold voltage increases in the temperature range of the smectic phase. One can see the temperature dependence of the threshold voltage in the literatures [24–26] for similar experiments.

Figure 5 illustrates the plots of conductance–voltage of the 6CB/8CB/8OCB mixture at different frequencies. As seen in Fig. 5, conductance values are fixed to a certain voltage and then increases above the threshold voltage, and again tend to be constant. The electrical conductivity of the liquid crystals increases with voltage frequency applied. The parallel conductivity $\sigma_\parallel$ values of the 6CB/8CB/8OCB mixture are higher than the perpendicular conductivity $\sigma\perp$ values.

Liquid crystal mixtures with a positive dielectric anisotropy are used for displays and the image quality of liquid crystal displays highly depends on the dielectric anisotropy of the liquid crystal [27]. The capacitance method was used for determination of the dielectric anisotropy and elastic constant values of 6CB/8CB/8OCB liquid crystal mixture. The capacitance method consists in the analysis of the voltage dependence of the capacity of the indium-tin oxide (ITO) coated planar nematic liquid crystal cell. The dielectric anisotropy for liquid crystals is expressed as

$$\Delta\varepsilon = \varepsilon_{||} - \varepsilon_{\perp}, \tag{1}$$

where $\varepsilon_\parallel$ and $\varepsilon_\perp$ are the parallel and perpendicular components of the electric permittivity, respectively. The dielectric anisotropy is calculated from capacitance experiments by eliminating the dielectric permittivity of the medium, ε, from Eq. (2):

$$C = \varepsilon_o.\varepsilon.\frac{A}{d}. \tag{2}$$

Here C is the capacitance value, ε_o and ε are dielectric permittivity values of free space and the medium, respectively, A is the cell plate area, and d is the thickness of the liquid crystal cell. After calculating the dielectric anisotropy $\Delta\varepsilon$ value, the splay elastic constant, K_{11}, is calculated by using Eq. (3):

$$K_{11} = \frac{\varepsilon_o \Delta\varepsilon V_{\text{th}}^2}{\pi^2}, \tag{3}$$

Table 2. The dielectric anisotropy Δ_ε and the splay elastic constant K_{11} values for 6CB/8CB/8OCB liquid crystal mixture at different frequencies.

Frequency (kHz)	V_{th} (V)	$\varepsilon_\parallel$	$\varepsilon_\perp$	$\Delta\varepsilon$	K_{11} (pN)
200	7.5	30.8	11.3	19.5	984.56
300	7.1	28.9	9.45	19.45	880.08
400	5.9	27.1	7.91	19.19	599.60
500	4.5	23.2	5.6	17.6	319.90

where V_{th} is the threshold voltage. The dielectric anisotropy $\Delta\varepsilon$ and the splay elastic constant K_{11} values for 6CB/8CB/8OCB liquid crystal mixture were calculated and presented in Table 2. As seen in Table 2, while the frequency increases, the dielectric anisotropy and splay elastic constant values decrease. One can see similar results in the literatures [23–29].

Absorption spectroscopic methods of analysis are based upon the fact that compounds absorb light radiation of a specific wavelength. In the analysis, the amount of light radiation absorbed by a sample is measured. The absorbance varies linearly with both the cell path length (l) and the concentration of the solution (c). These two relationships can be combined to yield a general equation called Beer's Law [30]. The Beer Law is given by Eq. (4):

$$A = \varepsilon cl, \tag{4}$$

where ε is the molar absorptivity. The molar absorptivity varies with the wavelength of light used in the measurement. The UV absorption spectra of mixtures of liquid crystals 6CB, 8CB, and 8OCB in chloroform solutions were measured between 200 and 400 nm. Figure 6 presents the obtained absorbance (A) spectra within 240 and 400 nm. The *trans–cis* conformation change of the 6CB/8CB/8OCB liquid crystal mixture can be evidenced by the change of its absorption spectra upon exposure to UV light at the wavelength in the region of the maximum absorption [31]. The 6CB/8CB/8OCB spectrum presents a maximum absorption corresponding to the $\pi-\pi*$ transition of the *trans* form at 286 nm, in agreement with maximum absorption wavelength (λ_{max}) reported in literatures [32,33], as well as E7 liquid crystal. The spectra of binary mixtures also exhibit strong absorption bands between 276 and 290 nm, like pure 6CB, 8CB, and 8OCB. The molar absorptivity ε values of the liquid crystal mixtures were calculated using Eq. (4). The obtained values, ε and λ_{max}, are given in Table 3. As seen
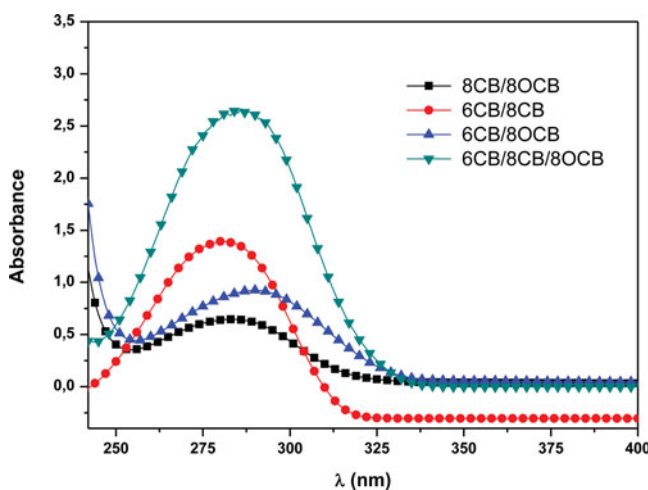
Figure 6. Observed UV spectra of the mixtures of liquid crystals 6CB, 8CB, and 8OCB.

Table 3. Molar absorptivity (ε) and wavelength (λ_{max}) of the mixtures of liquid crystals 6CB, 8CB, and 8OCB.

LC mixture	λ_{max} (nm)	ε ($M^{-1}cm^{-1}$)
8CB/8OCB	283	4.9×10^4
6CB/8CB	280	6.9×10^4
6CB/8OCB	290	5.8×10^4
6CB/8CB/8OCB	286	9.1×10^4

in Table 3, the molar absorptivity value of the 6CB/8CB/8OCB mixture is higher than the absorptivity values of the binary mixtures due to the alkyl chain length with H-aggregation and oxygen atom subsistence.

4. Conclusions

In this study, the thermo-electro-optic properties of the liquid crystal 6CB/8CB/8OCB mixture were investigated. DSC curves recorded to determine the phase transition temperatures showed different transition peaks in liquid crystal 6CB/8CB/8OCB mixture during continuous heating. The nematic range of the 6CB/8CB/8OCB mixture is the widest, with a 22.55 °C temperature range, among the liquid crystals 6CB, 8CB, 8OCB, and their mixtures. Morphological textures of phase transitions of liquid crystal mixtures were investigated by POM during continuous heating. It was observed that the phase transition temperature values obtained in the DSC experiments were in line with the phase transition temperature values observed in the POM experiments. The plots of capacitance–voltage of the 6CB/8CB/8OCB mixture indicated a threshold voltage. The dielectric anisotropy $\Delta \varepsilon$ and the splay elastic constant K_{11} values for 6CB/8CB/8OCB liquid crystal mixture were calculated, and this mixture showed an extremely large positive dielectric anisotropy. Also, the parallel conductivity $\sigma_{\parallel}$ values of the 6CB/8CB/8OCB mixture are higher than the perpendicular conductivity $\sigma_{\perp}$ values. The UV measurements showed that the properties of the 6CB/8CB/8OCB mixture to be characteristic of LC molecules in chloroform. The molar absorptivity ε was calculated by using the Beer Law. The molar absorptivity value of the 6CB/8CB/8OCB mixture was found to be higher than the absorptivity values of the binary mixtures due to the alkyl chain length with H-aggregation and oxygen atom subsistence.

Acknowledgments

References

[1] Javadian, S., Dalir, N., Gilani, A. G., Kakemam, J., & Yousefi, A. (2015). *J. Chem. Thermodynam.*, *80*, 22.
[2] Sharma, D. (2012). *J. Therm. Anal. Calorim.*, *109*, 331.
[3] Sharma, D., MacDonald, J. C., & Iannacchione, G. S. (2006). *J. Phys. Chem. B.*, *110*, 16679.
[4] Thoen, J., Marynissen, H., & Van Dael, W. (1982). *Phys. Rev. A*, *26*, 2886.
[5] Hegmann, T., Qi, H., & Marx, V. M. (2007). *J. Inorg. Organomet. Polym. Mater.*, *17*, 483.
[6] Cseh, L., & Mehl, G. H. (2007). *J. Mater. Chem.*, *17*, 311.
[7] Yilmaz, S. (2008). *Mater. Chem. Phys.*, *110*, 140.
[8] Yilmaz, S., & Bozkurt, A. (2008). *Mater. Chem. Phys.*, *107*, 410.
[9] Kima, B., Uma, Y. J., Jeona, S., Kikuchih, H., & Honga, S. K. (2014). *Liq. Cryst.*, *41*, 1619.

[10] Nesrullajev, A. (2014). *J. Mol. Liq.*, *196*, 217.

[11] Motosuke, M., & Nagasaka, Y. (2008). *Int. J. Thermophys.*, *29*, 2025.

[12] Vanbrabant, P. J. M., Dessaud, N., & Strömer, J. F. (2008). *Appl. Phys. Lett.*, *92*, 091101.

[13] Liang, D., & Leheny, R. L. (2007). *Phys. Rev. E*, *75*, 031705.

[14] Czub, J., Urban, S., & Würflinger, A. (2006). *Liq. Cryst.*, *33*, 85.

[15] M/s. Liquid Crystals Catalogue BDH Chemicals Limited Company. (2000). Poole, BH12 4NN, England.

[16] Özgan, Ş., & Okumuş, M. (2011). *Braz. J. Phys.*, *41*, 118.

[17] Okumus, M., & Ozgan, S. (2013). *Asian J. Chem.*, *25*, 3879.

[18] Fujimura, S., Yamamura, Y., Hishida, M., Nagatomo, S., & Saito, K. (2014). *Liq. Cryst.*, *41*, 927.

[19] Lafouresse, M. G., Sied, M. B., Allouchi, H., López, D. O., Salud, J., & Tamari, J. L. I. (2003). *Chem. Phys. Lett.*, *376*, 188.

[20] Czub, J., Gubernat, U., Gestblom, B., Dąbrowski, R., & Urban, S. (2004). *Z. Naturforsch.*, *59*, 316.

[21] Cladis, P. E., Guillon, D., Bouchet, F. R., & Finn, P. L. (1981). *Phys. Rev. A*, *23*, 2594.

[22] Gray, G. W., & Goodby, J. W. (1984). *Smectic Liquid Crystals – Textures and Structures*, Leonard Hill: London.

[23] Yakuphanoglu, F., Bilgin-Eran, B., Ocak, H., & Oweimreen, G. A. (2007). *Physica B: Condens. Matter*, *393*, 270.

[24] Czechowski, G., & Jadżyn, J. (2004). *Acta Phys. Pol. A*, *106*, 475.

[25] Abe, K., Usami, A., Ishida, K., Fukushima, Y., & Shigenari, T. (2005). *J. Korean Phys. Soc.*, *46*, 220.

[26] Neeraj, Kumar, P., & Raina, K. K. (2011). *J. Mater. Sci. Technol.*, *27*, 1094.

[27] Yakuphanoglu, F., Okutan, M., Köysal, O., & Keum, S. R. (2008). *Dyes Pigments*, *76*, 202.

[28] San, S. E., Okutan, M., Köysal, O., & Ono, H. (2005). *J. Non-Cryst. Solids*, *351*, 2764.

[29] Al-Hazmi, F., Al-Ghamdi, A. A., Al-Senany, N., Alnowaiser, F., & Yakuphanoglu, F. (2014). *Compos. Part B: Eng.*, *56*, 15.

[30] Ingle, J. D. J., & Crouch, S. R. (1988). *Spectrochemical Analysis*, Prentice Hall: Englewood Cliffs, NJ.

[31] Sridevi, S., et al. (2011). *Mater. Chem. Phys.*, *130*, 1329.

[32] Neuenfeld, S., & Schick, C. (2006). *Thermochim. Acta*, *446*, 55.

[33] Wu, S. T. (1991). *J. Appl. Phys.*, 69, 2080.